# Conformational states of annexin VI in solution induced by acidic pH

Marcin Golczak, Aneta Kirilenko, Joanna Bandorowicz-Pikula, Slawomir Pikula*

*Department of Cellular Biochemistry, Nencki Institute of Experimental Biology, 3 Pasteur Street, 02-093 Warsaw, Poland*

Received 13 February 2001; revised 10 April 2001; accepted 10 April 2001

First published online 19 April 2001

Edited by Gunnar von Heijne

**Abstract Acidic pH-induced folding of annexin (Anx)VI in solution was investigated in order to study the mechanism of formation of ion channels by the protein in membranes. Using 2-(*p*-toluidino)naphthalene-6-sulfonic acid as a hydrophobic probe, it was demonstrated that AnxVI exerts a large change in hydrophobicity at acidic pH. Moreover, circular dichroism spectra indicated that the native state of AnxVI changes at acidic pH towards a state characterized by a significant loss of α-helix content and appearance of new β-structures. These changes are reversible upon an increase of pH. It is postulated that the structural folding of AnxVI could explain how a soluble protein may undergo transition into a molecule able to penetrate the membrane hydrophobic region. The physiological significance of these observations is discussed. © 2001 Published by Elsevier Science B.V. on behalf of the Federation of European Biochemical Societies.**

*Key words:* Annexin VI; Steady-state fluorescence; Circular dichroism; pH-induced folding

## 1. Introduction

Annexin (Anx)VI [1,2], a member of a family of homologous $Ca^{2+}$- and phospholipid-binding proteins is expressed in two isoforms in mammalian tissues. Both isoforms interact with membranes enriched with phosphatidylserine (PtdSer) at neutral pH in a $Ca^{2+}$-dependent manner [3]. The larger isoform of AnxVI contains 673 amino acids with a $M_r$ of 68 kDa and p*I* of 5.8 [4,5]. The crystal structures of AnxVI in soluble (human) [6] and membrane-bound (bovine) [7] form have been solved, indicating that $Ca^{2+}$ does not produce a major conformational change in AnxVI under physiological pH and ionic strength. Recently, it was found that porcine liver AnxVI, which is similar to its human counterpart [8], is able to bind to phospholipid bi- and monolayers in a $Ca^{2+}$-independent manner, stimulated by acidic pH (half-maximal binding to asolectin liposomes occurred at pH 5.3) [9]. The binding was accompanied by the formation of voltage-dependent non-specific ion channels by AnxVI with a single channel conductance of 24 pS under symmetric conditions (50 mM CsCl), as determined by the black lipid membrane technique [9]. As a mechanism of channel formation, it has been proposed that AnxVI undergoes profound changes of its native structure that are accompanied by an increase in the overall hydrophobicity of the protein [9].

In the present report we have tested this hypothesis by using fluorescence and far-UV circular dichroism (CD) measurements. With this experimental approach we observed a profound increase of protein hydrophobicity at acidic pH and the appearance of an AnxVI conformational state that varies from the native AnxVI structure near pH 7.0. Such behavior may explain the existence of $Ca^{2+}$-independent isoforms of AnxVI that were observed by other investigators within the cells to behave as membrane integral proteins [10–13].

## 2. Materials and methods

### 2.1. Chemicals

PtdSer, *N*-acetyl-L-tryptophan amide and 2-(*p*-toluidino)naphthalene-6-sulfonic acid (TNS) were purchased from Sigma-Aldrich (Poznan, Poland). All other chemicals were of the highest purity commercially available.

### 2.2. Preparation of porcine liver AnxVI

The fraction of $Ca^{2+}$-binding proteins enriched in AnxVI was isolated from porcine liver homogenate by means of $Ca^{2+}$ precipitation. Further purification of AnxVI to homogeneity was achieved using ion exchange chromatography, as previously described [8,14]. The protein was lyophilized and stored at −20°C until use. Protein purity was verified by sodium dodecyl sulfate–polyacrylamide gel electrophoresis (SDS–PAGE) and monoclonal antibodies against human AnxVI (Signal Transduction Laboratories, Lexington, KY, USA) that recognized the porcine liver AnxVI isoform. In addition, some proteolytic fragments of AnxVI were directly sequenced after electroblotting onto polyvinylidene difluoride membranes, confirming its identity [8].

### 2.3. Steady-state fluorescence measurements

All fluorescence and light scattering measurements described in this report were performed with the aid of a Fluorolog 3 Spectrometer (SPEX) at 25°C in a quartz cuvette of 5 mm optical pathlength. The following buffers were used: 10 mM citric buffer in the pH range from 3.0 to 6.2, or 10 mM Tris–HCl buffer in the pH range from 7.0 to 8.3, supplemented with 50 mM NaCl and 0.1 mM EGTA. These buffers are called citric or Tris–HCl throughout the text.

The fluorescence emission spectra of TNS in the presence or absence of AnxVI were recorded between 350 and 570 nm at 25°C with $\lambda_{ex} = 345$ nm [15]. For TNS alone, the $\lambda_{max}$ of emission amounted to 490 nm. Both emission and excitation slits were set at 0.5 nm. TNS concentrations varied from 0 to 30 μM at a fixed protein concentration (1 μM).

Fluorescence resonance energy transfer (FRET) was determined by recording fluorescence emission spectra of AnxVI Trp residues (a donor) in the presence of various concentrations of TNS (an acceptor) from 0 to 30 μM. The pH of the assay medium varied from pH 3.0 to 8.3. Samples were excited at $\lambda_{ex} = 295$ nm, with emission and excitation slits set at 1 nm. The donor and acceptor fluorescence emission intensities were recorded in the wavelength range from 300 to 500 nm at 1 nm intervals. The energy transfer efficiency (*E*) was calculated on

*Corresponding author. Fax: (48)-22-822 5342.
E-mail: slawek@nencki.gov.pl

*Abbreviations:* Anx, annexin; CD, circular dichroism; FRET, fluorescence resonance energy transfer; PtdSer, phosphatidylserine; SDS–PAGE, sodium dodecyl sulfate–polyacrylamide gel electrophoresis; TNS, 2-(*p*-toluidino)naphthalene-6-sulfonic acid

0014-5793/01/$20.00 © 2001 Published by Elsevier Science B.V. on behalf of the Federation of European Biochemical Societies.
PII: S0014-5793(01)02402-4

the basis of the following equation: $E = 1-(N_{DA}/N_D)$, where $N_D$ is the fluorescence efficiency of the donor and $N_{DA}$ is the fluorescence efficiency of the donor in the presence of an acceptor [16].

To determine the intrinsic fluorescence of AnxVI as a function of pH, the emission spectra of AnxVI (0.2 μM) were monitored at 25°C with a 2 nm spectral resolution for both excitation and emission, in the wavelength range from 300 to 400 nm at a pH range from 3.0 to 8.3 ($\lambda_{ex} = 295$ nm). Under the same conditions, the emission spectra of *N*-acetyl-L-tryptophan amide in a concentration range corresponding to the concentration of AnxVI Trp residues were also recorded. They revealed no pH-sensitivity, as already described in [17].

Light scattering of AnxVI in solution was measured in order to determine protein aggregation. Scattered light at 90° was collected between 360 and 400 nm (in 10 nm steps). The assay medium contained 0.02 or 0.2 mg/ml of AnxVI in citric or Tris–HCl buffers, supplemented with NaCl and EGTA.

### 2.4. CD measurements

The far-UV CD spectra of AnxVI were collected at 25°C using an AVIV CD spectrophotometer (AVIV Associates, USA) in a 5 mm optical pathlength quartz cuvette. The assay media contained citric (pH 3.0–6.2) or Tris–HCl (pH 7.0–8.3) buffers, 0.2 mg/ml of AnxVI, 50 mM NaCl and 0.1 mM EGTA. Each spectrum was recorded as an average of six scans between 190 and 260 nm. Participation of α-helix and β-sheet structures in protein secondary structure was calculated with the aid of Contin software (1999 edition).

### 2.5. Other procedures

The protein concentration was determined according to the Bradford method [18], with bovine serum albumin as a standard. SDS–PAGE (reducing conditions) was performed on 6% stacking and 12% resolving gels; gels were stained with Coomassie brilliant blue [19].

## 3. Results

Using TNS as a hydrophobic probe, it was determined that the hydrophobicity of AnxVI increases upon acidification of the assay medium. The binding of TNS to AnxVI is evidenced by a significant enhancement of TNS fluorescence intensity and a remarkable blue shift of its fluorescence emission $\lambda_{max}$ from 490 nm in the absence of protein to 427 nm in the presence of AnxVI (Fig. 1A). These changes were markedly dependent on pH, with a midpoint of the titration at pH 5.5. It is worth stressing that the fluorescence of TNS alone was independent of pH, in the pH range studied, as also reported by Kachel et al. [20].

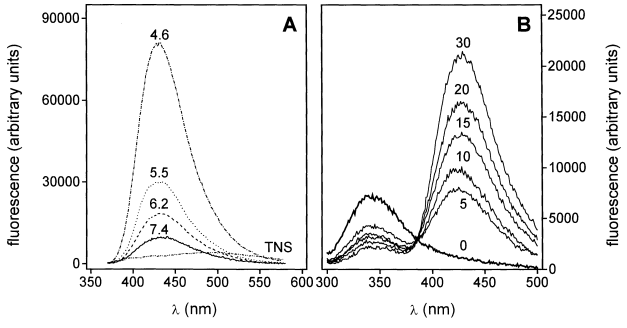


Fig. 1. TNS binding to porcine AnxVI. A: The protein (1 μM) was dissolved in either citric buffer (pH 3.0–6.2) or Tris–HCl buffer (pH 7.4–8.3). The TNS emission spectra ($\lambda_{ex} = 345$ nm) in the presence of AnxVI were determined at pH 7.4 (solid line), 6.2 (dash line), 5.5 (dot line) and 4.6 (dot–dash line). The spectrum of 5 μM TNS without AnxVI is also shown (short dash–dot line). B: Typical fluorescence emission spectra of AnxVI (1 μM) in the presence of various TNS concentrations (from 0 to 30 μM) demonstrate FRET between donor (AnxVI Trp residues, excited at $\lambda_{ex} = 295$ nm) and acceptor (TNS, emission peak at $\lambda_{em} = 427$ nm) at pH 4.6.

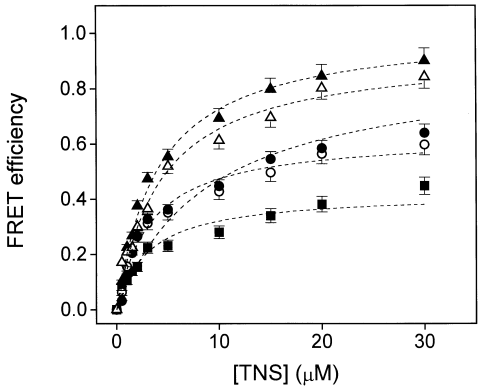


Fig. 2. pH-dependence of FRET efficiency. FRET was determined in the presence of 1 μM AnxVI and TNS concentrations varying from 0 to 30 μM. The pH values of the assay media were as follows: pH 8.0 (filled squares), pH 6.2 (open circles), pH 5.0 (filled circles), pH 4.0 (open triangles) and pH 3.0 (filled triangles). The FRET efficiency was calculated from the spectra determined as in Fig. 1B, using the equation given in Section 2. The mean values ± S.D. from three experiments are shown.

The binding of TNS was accompanied by FRET from excited Trp residues of AnxVI to TNS at low pH. FRET is evidenced from the quenching of AnxVI fluorescence intensity at pH 4.6 in the presence of increasing concentrations of TNS (Fig. 1B). The results of the reciprocal experiment, i.e. determination of FRET at fixed concentrations of AnxVI and TNS but various pH values (from pH 3.0 to 8.3) or titration of TNS with various AnxVI concentrations, resulted in the same conclusion that significant FRET occurs only at acidic pH, while at pH 7.4 FRET was negligible (not shown). These experiments revealed that FRET is the result of TNS–AnxVI interactions but not changes in the fluorescence properties of the protein. FRET efficiency depended on pH and TNS concentration (Fig. 2), pointing to the existence of an AnxVI state with higher protein hydrophobicity than the native state at pH 7.4–8.0, with a low degree of hydrophobicity. If the changes in AnxVI hydrophobicity at acidic pH are due to a pH-dependent conformational change of the protein, then this change should be revealed by fluorescence and CD spectroscopies. Both techniques were used in this study to analyze the secondary structure of AnxVI and the potential changes of environment of the aromatic Trp residues of the protein.

To test the latter presumption, the fluorescence of two reporter Trp residues in the AnxVI molecule, $Trp^{192}$ and $Trp^{343}$, was measured as a function of pH. In Fig. 3A, three typical fluorescence emission spectra are shown, revealing that a drop in pH of the assay medium is associated with the decrease of Trp fluorescence at pH 3.0 (by 45% in comparison to pH 8.0) and a shift of the maximum of the AnxVI emission spectrum to longer wavelengths, from $\lambda_{max} = 336$ nm at pH 8.0 to 340 nm at pH 4.6 and 346 nm at pH 3.0. Moreover, AnxVI spectra at various pH values relate the magnitude of the red shift of emission spectrum to decreasing pH values (Fig. 3B). This suggests that the tertiary structure of AnxVI at various pH values varies from each other by the exposure of Trp residues to the surrounding milieu. In addition, while the intrinsic fluorescence maximum shifts from $\lambda_{em} = 336$ nm to 346 nm upon acidification of the assay medium and the absence of TNS (Fig. 3B), such a shift is not observed in the presence of hydrophobic probe ($\lambda_{max} = 336$ nm). This observation could

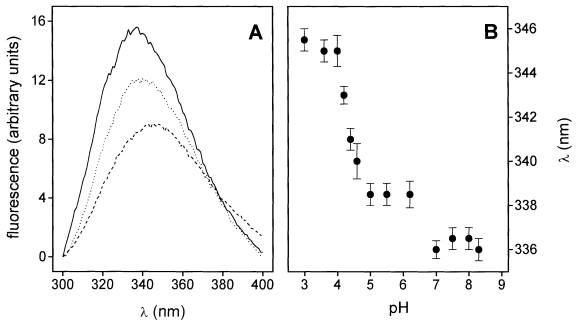


Fig. 3. The pH-dependent blue shift of the fluorescence emission maximum of the Trp residues of AnxVI. A: The emission spectra ($\lambda_{ex}$ = 295 nm) were measured at pH 3.0 (dashed line), pH 4.6 (dotted line) and pH 8.0 (solid line) at 25°C in 10 mM buffers, supplemented with 50 mM NaCl and 0.1 mM EGTA. The protein concentration was 0.2 μM. B: The maxima of fluorescence emission spectra of AnxVI in the pH range shown in the abscissa to the figure were determined under the same conditions as described in (A) in triplicate. The mean values of $\lambda_{max}$ ± S.D. of fluorescence emission spectrum are plotted. The data resolution was 1 nm.

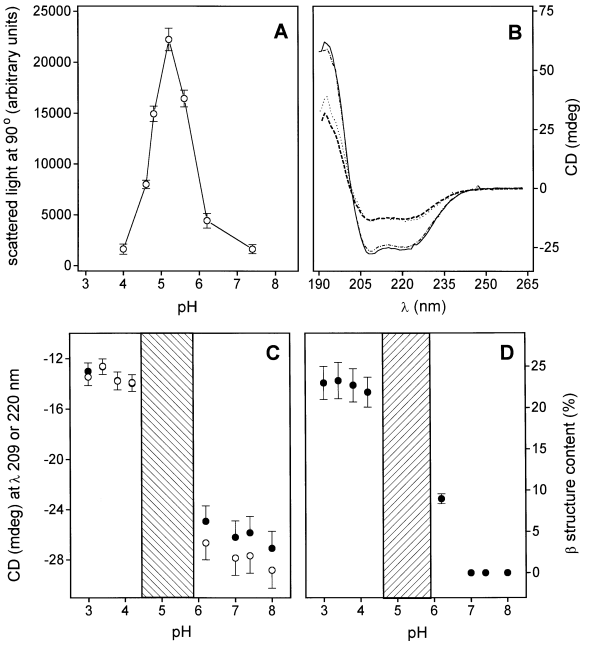


Fig. 4. The effect of pH on the aggregation of AnxVI in solution and its secondary structure. A: The ability of AnxVI solutions to scatter UV light at 25°C was determined under conditions described in Section 2. The light wavelength was fixed at 400 nm. The AnxVI concentration was 0.2 mg/ml, i.e. 2.9 μM. The mean values from three determinations ± S.D. are shown. B: Typical far-UV CD spectra of AnxVI at different pH values were measured at 25°C. The assay medium (of total volume 0.5 ml) contained 0.1 mg of AnxVI in a buffer of pH 8.0 (solid line), pH 6.2 (dot–dash line), pH 4.0 (dotted line) or pH 3.0 (dash line). C: Values of CD signals of AnxVI at λ 222 nm (open circles) and 209 nm (filled circles), corresponding to signals characteristic for α-helix structures, are plotted. D: The β-structure content of AnxVI was calculated from the spectra depicted in (B) with the aid of Contin software. The pH values ranged from 3.0 to 8.0. The mean values ± S.D. from at least three determinations are depicted in (C) and (D). The hatched area represents the pH value range from 4.8 to 5.9 where we were unable to accurately record the CD spectra of AnxVI due to protein aggregation.

be due to a shielding effect, however, it is also valid that FRET, upon binding of TNS to AnxVI, occurred in the vicinity of AnxVI Trp residues and that this may prevent a red shift of Trp fluorescence upon acidification of the assay medium.

Due to the tendency of various proteins to aggregate at acidic pH, the pH-dependent aggregation profile of AnxVI was determined using light scattering at 90° of a protein solution as a function of pH (Fig. 4A). The determinations revealed that, in the pH range from 4.8 to 5.8 (including the p*I* value of AnxVI), AnxVI in solution tends to aggregate, although, the aggregation is reversible by raising the pH above 6.0 or by lowering it below 4.0. The absence of significant light scattering at a pH below 4.0 does not preclude the possibility of formation of AnxVI oligomers, due to the tendency of Anxs to interact with each other on the membrane surface [21–24].

To follow conformational transitions of the protein induced by acidic pH, we have determined the far-UV CD spectra of AnxVI as a function of pH. Except pH values ranging from pH 4.8 to pH 5.9, it was possible to measure the CD spectra of AnxVI at pHs below 4.0 and above 6.0 (Fig. 4B). These spectra allowed us to distinguish two secondary structure states of AnxVI, as shown in Fig. 4C,D. These states differ from each other by the values of ellipticity (expressed in mdeg) of protein determined at $\lambda$ equal to 209 and 222 nm, i.e. the determinants of α-helix structures of protein (Fig. 4C). In parallel, we observed that lowering the pH of the assay medium results not only in a drop of α-helix content (both regular and distorted α-helices [25]) of AnxVI from 88.2% at pH 7.4 to 50.7% at pH 3.0 (Table 1) but also in the formation of new β-structures; their content changed from 1.2% at pH 7.4 to 23.2% at pH 3.0 (Table 1, Fig. 4D). This was accompanied by a reduction of the number of segments within the Anx molecule, from 8.2 segments per 100 residues at pH 7.4 to 4.8 segments per 100 residues at pH 3.0. The number of segments calculated on the basis of CD determinations at pH 7.4 is 29% larger than the number of segments obtained from analysis of crystal structure of AnxVI (5.8 per 100 residues) [6]. Surprisingly, the average length of these segments did not

Table 1
The effect of pH on a secondary structure of AnxVI

| pH | Regular α-helix | Distorted α-helix | Regular β-strands | Distorted β-strands | Turns | Unordered structures |
|---|---|---|---|---|---|---|
| 3.0 | 31.2 ± 1.2 | 19.5 ± 0.9 | 12.2 ± 1.5 | 11.0 ± 0.9 | 12.3 ± 2.4 | 13.9 ± 1.7 |
| 4.2 | 32.2 ± 0.8 | 17.7 ± 0.8 | 12.0 ± 1.2 | 10.3 ± 1.2 | 12.5 ± 2.6 | 13.2 ± 1.6 |
| 6.2 | 42.8 ± 4.1 | 26.2 ± 4.2 | 1.0 ± 1.0 | 6.8 ± 3.2 | 4.9 ± 1.1 | 8.3 ± 1.0 |
| 7.4 | 67.1 ± 4.5 | 21.1 ± 3.4 | 0.1 ± 0.1 | 1.1 ± 0.6 | 2.6 ± 0.7 | 7.8 ± 0.9 |

Calculations are based on the CD spectra measured under the conditions detailed in the legend to Fig. 4B. The mean values ± S.D. from at least three determinations are shown and were calculated with the aid of Contin software. Distorted structures, according to the definition given in the software description, are related to the structures that are characterized by deviations from ideal conformational angles, leading to distortions in the secondary structure such as bends, twists, end frying, etc. [25].

change much as a function of pH: from 13.9 residues per segment at pH 7.4 to 11.2 residues per segment at pH 3.0. These results, taken together, indicate that a significant secondary structure of AnxVI persists even at acidic pH, and acidification is not accompanied by denaturation of protein, as also examined previously with the use of Fourier transformed infrared spectroscopy [9].

## 4. Discussion

This report provides evidence of a $Ca^{2+}$-independent increase in the level of exposed hydrophobic surface of AnxVI at low pH. In this respect, AnxVI is similar to other members of the Anx family of proteins (AnxV and AnxXII) [26–28]. The changes in hydrophobic surface of AnxVI accompany the $Ca^{2+}$-independent formation of ion channels by AnxVI at acidic pH (with a single channel conductance of 23 pS [9]) and a $Ca^{2+}$-independent conformational change resulting in the conversion of α-helical (−38.3% at pH 4.2, Table 1) to β-sheet structure (+21.1% at pH 4.2, Table 1). In addition, far-UV CD data show that the number of α-helical segments in AnxVI is lowered by pH and the average length of the remaining α-helical segments does not change. Together, the described and reported properties of AnxVI appear connected to the membrane-bound $Ca^{2+}$-independent forms of the protein that can only be removed from the membrane bilayer by detergent solubilization [10–13]. The ability of AnxVI to bind $Ca^{2+}$ declines with lower pH, in accordance with all the $Ca^{2+}$-independent properties of AnxVI [9]. Any proposed mechanism describing the low pH, $Ca^{2+}$-independent behavior of AnxVI must take into account these properties and the cellular localization, known links to disease and potental functional pathways of AnxVI. Knowledge acquired from unrelated proteins with similar properties may provide further clues.

AnxVI associates specifically with membranes of low pH compartments (i.e. late endosomes and synaptosomes) in a number of cell types, indicating a role of AnxVI at late stages of the endocytic pathway [29–31]. It has been recently shown that the membrane association of endosomal coat proteins (COPs), involved in membrane transport in the endocytic pathway, depends on an acidic endosomal pH. It was found that membrane recruitment of endosomal COPs depends on a small cytosolic GTP-binding protein, ARF1. The membrane association of ARF1 is sensitive to the endosomal pH, perhaps through a binding to a transmembrane protein that changes its conformation on the cytosolic side of the endosome membrane upon acidification of the endosome lumen [32]. Therefore, ARF1 acts as the cytosolic component of a transmembrane pH-sensing mechanism [32]. It can be speculated that AnxVI also reveals transmembrane pH-sensing properties that may explain the preferential binding of AnxVI to late endosomes characterized by an acidic interior. However, in contrast to ARF1, AnxVI probably does not require additional endosomal protein for binding to endosome membrane, being itself a pH-dependent protein. If so, it is possible that under physiological conditions AnxVI may sense lower pH values than in the cytosol.

How and where do such areas of low pH arise inside the cell? A possible explanation can be provided by the observation made by Van der Goot et al. [33] who studied the interaction of colicin A with membranes made of anionic phospholipids. They found the local pH value near the surface of such membranes is lower than in the cytoplasm by 1.6 pH units [33]. Taking into account that AnxVI preferentially interacts with membranes enriched with acidic phospholipids [34], one may consider a similar sensitivity of AnxVI for a lower interfacial pH as that described for colicin A. It must be stressed, however, that the half-maximal association of AnxVI with lipid bilayers occurs in vitro at pH 5.3 [9], i.e. in a pH range outside cytosolic pH variations. On the other hand, membrane integration of AnxVI may occur at localized areas of higher $H^+$ concentrations connected with membrane lipid microdomains consisting of acidic phospholipids and/or their protein components.

The low pH-sensitivity of AnxVI could be of particular importance under pathological or stressful conditions. For example, the pH inside muscle fibers can decline from pH 7.1 to pH 6.5 due to skeletal muscle fatigue [35]. This change affects the function of $Ca^{2+}$-transport systems, as observed for the rabbit skeletal muscle ryanodine receptor that was in vitro inhibited with a half-inhibitory cytoplasmic pH of 6.5 [36]. Intracellular acidosis is also a recognised result of ischemia. In one experimental system of ischemia, the result was decreased insulin signalling through the influence of tyrosine phosphorylation of the insulin receptor and changes in the activity of various kinases [37]. Anxs were not directly implicated in this study. However, Anxs do participate in insulin secretion through various mechanisms and may also become targets in ischemia. For example, anti-AnxXI antibodies were found to inhibit insulin secretion from pancreatic β-cells [38] and the heterozygous anx7 (+/−) mouse phenotype was associated with a substantial defect in insulin secretion [39]. AnxVI is also involved in other secretion pathways, for example, AnxVI was found secreted from hepatocytes into bile [40].

Ischemia also accompanies programmed cell death (apoptosis) and multidrug resistance of various cell lines that are characterized by changes in intracellular pH gradients that affect the accumulation, secretion and endocytosis of anti-cancer drugs [41]. It was shown that apoptosis of murine thymocytes, induced by extracellular ATP, is accompanied with a rapid intracellular acidification (by 0.3 pH units) [42], and apoptosis of rat superior cervical ganglion cells in vitro, induced by $Na^+$ overload, results in a pH drop to 6.5 [43]. These observations, if AnxVI would be involved, imply the transformation of part of AnxVI from a cytosolic to membrane integral protein.

The question remains what is the molecular mechanism for extrusion of AnxVI into the membrane hydrophobic core. Changes of pH evoked aggregation of AnxV and folding of its domain III, which contains the $Trp^{187}$ residue that plays a role in Anx-membrane binding [44,45]. For AnxV and hydra AnxXII, pH-induced changes in protein hydrophobicity [26,27] were accompanied by the insertion of these proteins into lipid bilayers and the formation of ion channels [27,46]. In addition, for hydra AnxXII, acidic pH-induced oligomerization was found of importance for its channel activity [28,46] while for AnxV, playing a role in the calcification of the matrix, changes in protein hydrophobicity were indispensable for pH-induced membrane insertion of the protein [26]. In contrast to the pH-induced changes observed for AnxV [17,26,43,47], AnxVI undergoes larger conformational changes and the transition of the native to low pH-induced state is already observed at pH 6.2.

The structural transition involving the rearrangement from

α-helix-rich to β-structure-rich state, as described in this report for AnxVI, was also observed for a cytolytic exotoxin from *Clostridium perfringens*, perfringolysin O. This toxin binds to cholesterol-rich membranes and self-associates to form aqueous pores. The cholesterol-dependent conversion of the toxin to a membrane-bound oligomeric form involves the formation of a large prepore complex and transition in which at least four α-helices unfold to form a membrane-spanning amphipathic β-sheet [48–50]. A similar pH-dependent conversion was described for cellular prion protein, $PrP^C$. The conversion from monomeric $PrP^C$ to an infectious agent of transmissible spongiform encephalitis, e.g. oligomeric prion protein, was found to be characterized by a decrease in α-helical structure and increase in β-sheet content, and the formation of amyloid [51]. The stable intermediate of prion protein upon acidification was rich in β-sheet structures [52]. It is possible that the formation of new β-structures in the AnxVI molecule is responsible for membrane insertion of the Anx. However, in the case of the transmembrane form of recombinant hydra AnxXII, detected by site-directed spin labeling, it was found that upon insertion at the membrane a continuous transmembrane α-helix is formed from a helix–loop–helix motif (within the Anx fold). It was proposed that the corresponding long helices come together to form an aqueous pore [45]. No evidence for such a transition was observed from the far-UV CD spectra of AnxVI. These spectra were determined, however, in solution. Work is in progress in our laboratory to further characterize the mechanism of pH-induced conformational transitions within the AnxVI molecule upon membrane insertion. We will also search for target molecules of AnxVI and physiological processes under which pH-induced changes in AnxVI properties may play a regulatory role.

*Acknowledgements:* This work was supported by Grant No. 6 PO4A 027 14 from the State Committee for Scientific Research (for J.B.-P.). The authors wish to thank P. Groves and A. Kasprzak from the Nencki Institute of Experimental Biology, Warsaw, Poland, and R. Buchet from Université Claude Bernard-Lyon 1, Villeurbanne, France, for fruitful discussions.

## References

[1] Crompton, M.R., Owens, R.J., Totty, N.F., Moss, S.E., Waterfield, M.D. and Crumpton, M.J. (1988) EMBO J. 7, 21–27.
[2] Fan, H., Josic, D., Lim, Y.P. and Reutter, W. (1995) Eur. J. Biochem. 230, 741–751.
[3] Gerke, V. and Moss, S.E. (1997) Biochim. Biophys. Acta 1357, 129–154.
[4] Moss, S.E. and Crumpton, M.J. (1990) FEBS Lett. 261, 299–302.
[5] Kaetzel, M.A., Pula, G., Campos, B., Uhrin, P., Horseman, N. and Dedman, J.R. (1994) Biochim. Biophys. Acta 1223, 368–374.
[6] Benz, J., Bergner, A., Hofmann, A., Demange, P., Göttig, P., Liemann, S., Huber, R. and Voges, D. (1996) J. Mol. Biol. 260, 638–643.
[7] Avila-Sakar, A.J., Creutz, C.E. and Kretsinger, R.H. (1998) Biochim. Biophys. Acta 1387, 103–116.
[8] Bandorowicz-Pikula, J., Wrzosek, A., Danieluk, M., Pikula, S. and Buchet, R. (1999) Biochem. Biophys. Res. Commun. 263, 775–779.
[9] Golczak, M., Kicinska, A., Bandorowicz-Pikula, J., Buchet, R., Szewczyk, A. and Pikula, S. (2001) FASEB J. 10.1096/fj.00-0523fje.
[10] Bianchi, R., Giambanco, I., Ceccarelli, P., Pula, G. and Donato, R. (1992) FEBS Lett. 296, 158–162.
[11] Turpin, E., Russo-Marie, F., Dubois, T., de Paillerets, C., Alfsen, A. and Bomsel, M. (1998) Biochim. Biophys. Acta 1402, 115–130.
[12] Babiychuk, E.B., Palstra, R.J., Schaller, J., Kampfer, U. and Draeger, A. (1999) J. Biol. Chem. 274, 35191–35195.
[13] Lavialle, F., Rainteau, D., Massey-Harroche, D. and Metz, F. (2000) Biochim. Biophys. Acta 1464, 83–94.
[14] Bandorowicz-Pikula, J. and Awasthi, Y.C. (1997) FEBS Lett. 409, 300–306.
[15] Mani, R.S. and Kay, C.M. (1989) Biochem. J. 259, 799–804.
[16] Lakowicz, J.R. (1983) Principles of Fluorescence Spectroscopy, Plenum Press, New York.
[17] Beermann ofm cap, B.B., Hinz, H.J., Hofmann, A. and Huber, R. (1998) FEBS Lett. 423, 265–269.
[18] Bradford, M.M. (1976) Anal. Biochem. 72, 248–254.
[19] Laemmli, U.K. (1970) Nature (London) 227, 680–685.
[20] Kachel, K., Asuncion-Punzalan, E. and London, E. (1998) Biochim. Biophys. Acta 1374, 63–76.
[21] Mailliard, W.S., Luecke, H. and Haigler, H.T. (1997) Biochemistry 36, 9045–9050.
[22] Concha, N.O., Head, J.F., Kaetzel, M.A., Dedman, J.R. and Seaton, B.A. (1992) FEBS Lett. 314, 159–162.
[23] Zaks, W.J. and Creutz, C.E. (1991) Biochemistry 30, 9607–9615.
[24] Evans, T.C.Jr. and Nelsestuen, G.L. (1994) Biochemistry 33, 13231–13238.
[25] Sreerama, N., Venyaminov, S.Y. and Woody, R.W. (1999) Protein Sci. 8, 370–380.
[26] Köhler, G., Hering, U., Zschörnig, O. and Arnold, K. (1997) Biochemistry 36, 8189–8194.
[27] Isas, J.M., Cartailler, J.P., Sokolov, Y., Patel, D.R., Langen, R., Luecke, H., Hall, J.E. and Haigler, H.T. (2000) Biochemistry 39, 3015–3022.
[28] Cartailler, J.P., Haigler, H.T. and Luecke, H. (2000) Biochemistry 39, 2475–2483.
[29] Grewal, T., Heeren, J., Mewawala, D., Schnitgerhans, T., Wendt, D., Salomon, G., Enrich, C., Beisiegel, U. and Jackle, S. (2000) J. Biol. Chem. 275, 33806–33813.
[30] Pons, M., Ihrke, G., Koch, S., Biermer, M., Pol, A., Grewal, T., Jackle, S. and Enrich, C. (2000) Exp. Cell Res. 257, 33–47.
[31] Kamal, A., Ying, Y. and Anderson, R.G.W. (1998) J. Cell Biol. 142, 937–947.
[32] Gu, F. and Gruenberg, J. (2000) J. Biol. Chem. 275, 8154–8160.
[33] Van der Goot, F.G., Gonzáles-Mañas, J.M., Lakey, J.H. and Pattus, F. (1991) Nature (London) 354, 408–410.
[34] Hofmann, A., Benz, J., Liemann, S. and Huber, R. (1997) Biochim. Biophys. Acta 1330, 254–264.
[35] Fitts, R.H. (1994) Physiol. Rev. 74, 49–94.
[36] Laver, D.R., Eager, K.R., Taoube, L. and Lamb, G.D. (2000) Biophys. J. 78, 1835–1851.
[37] Beauloye, C., Bertrand, L., Krause, U., Marsin, A.S., Dresselaers, T., Vanstapel, F., Vanoverschelde, J.L. and Hue, L. (2001) Circ. Res. 88, 513–519.
[38] Iino, S., Sudo, T., Niwa, T., Fukasawa, T., Hidaka, H. and Niki, I. (2000) FEBS Lett. 479, 46–50.
[39] Srivastava, M., Atwater, I., Glasman, M., Leighton, X., Goping, G., Caohuy, H., Miller, G., Pichel, J., Westphal, H., Mears, D., Rojas, E. and Pollard, H.B. (1999) Proc. Natl. Acad. Sci. USA 96, 13783–13788.
[40] Thorin, B., Gache, G., Dubois, T., Grataroli, R., Domingo, N., Russo-Marie, F. and Lafont, H. (1995) Biochem. Biophys. Res. Commun. 209, 1039–1045.
[41] Belhoussine, R., Morjani, H., Sharonov, S., Ploton, D. and Manfait, M. (1999) Int. J. Cancer 81, 81–89.
[42] Nagy, P.V., Feher, T., Morga, S. and Matko, J. (2000) Immunol. Lett. 72, 23–30.
[43] Koike, T., Tanaka, S., Oda1, T. and Ninomiya, T. (2000) Brain Res. Bull. 51, 345–355.
[44] Sopkova, J., Vincent, M., Takahashi, M., Lewit-Bentley, A. and Gallay, J. (1998) Biochemistry 37, 11962–11970.
[45] Sopkova-De Oliveira Santos, J., Fischer, S., Guilbert, C., Lewit-Bentley, A. and Smith, J.C. (2000) Biochemistry 39, 14065–14074.
[46] Langen, R., Isas, J.M., Hubbell, W.L. and Haigler, H.T. (1998) Proc. Natl. Acad. Sci. USA 95, 14060–14065.
[47] Arboledas, D., Olmo, N., Lizarbe, M.A. and Turnay, J. (1997) FEBS Lett. 416, 217–220.

[48] Shepard, L.A., Heuck, A.P., Hamman, B.D., Rossjohn, J., Parker, M.W., Ryan, K.R., Johnson, A.E. and Tweten, R.K. (1998) Biochemistry 37, 14563–14574.
[49] Shepard, L.A., Shatursky, O., Johnson, A.E. and Tweten, R.K. (2000) Biochemistry 39, 10284–10293.
[50] Shatursky, O., Heuck, A.P., Shepard, L.A., Rossjohn, J., Parker, M.W., Johnson, A.E. and Tweten, R.K. (1999) Cell 99, 293–299.
[51] Hornemann, S. and Glockshuber, R. (1998) Proc. Natl. Acad. Sci. USA 95, 6010–6014.
[52] Swietnicki, W., Petersen, R., Gambetti, P. and Surewicz, W.K. (1997) J. Biol. Chem. 272, 27517–27520.